

Conductivity of two-dimensional electrons in a periodic potential in a strong magnetic field

G. R. Aizin and V. A. Volkov

Institute of Radio Engineering and Electronics, Academy of Sciences of the USSR, Moscow

(Submitted 23 April 1984)

Zh. Eksp. Teor. Fiz. **87**, 1469–1480 (October 1984)

Two-dimensional electrons in the inversion layer on a semiconductor surface with high Miller indices move in a weak one-dimensional periodic potential $V(x)$ whose period can be comparable with the magnetic length in realistic magnetic fields B . The potential $V(x)$ lifts partially the degeneracy of the Landau levels with respect to the center of the orbit, and forms one-dimensional magnetic bands. It is assumed that the magnetic-band width is large in comparison with the collisional broadening of the Landau levels, but small in comparison with the cyclotron energy. The conductivity σ_{ii} ($i = x, y$) over the ground magnetic band is found in the case of Born scattering by point impurities to be highly anisotropic and contains two contributions, namely, migrational and band contributions. The former is determined by the migration of the center of the cyclotron orbit and decreases with decreasing scattering. The latter is due to classical motion of the electron over the magnetic band and increases without limit as the scattering is reduced; it is nonzero only for σ_{yy} .

1. INTRODUCTION

Studies of the electronic properties of two-dimensional ($2D$) systems have largely been confined to inversion layers on separation boundaries of semiconductors.¹ Studies of $2D$ transport phenomena in quantized magnetic fields have become particularly topical since the discovery in such systems of the quantum Hall effect.² From the theoretical point of view, this problem is nowhere near a complete solution, even in the single-particle approximation, despite its rather long history.^{3–6} The basic difficulty is the infinitesimal width of Landau levels and the attendant absence of a small parameter associated with scattering. General results have been obtained only for systems in which a large number of Landau levels is filled. They are: the Hall conductivity σ_{xy} is quantized whereas the transverse conductivity σ_{xx} is zero.^{7–10} There are only two publications in which a rigorous analysis is given of arbitrary level filling. It is shown in Ref. 6 that $\sigma_{xx} = 0$ at zero temperature. It is not clear, however, to what extent this result depends on the particular model employed, namely, the model of σ -like impurities. The renormalization group was used in Ref. 11 to obtain a qualitative relationship between σ_{xx} and σ_{xy} in the general case.

The physical complexity of the problem is due to the following. On the one hand, the potential due to the impurities lifts the degeneracy of the Landau levels with respect to the center of the cyclotron orbit and produces a band of finite width. On the other hand, it also gives rise to transitions between states in the resulting band. Attempts to allow for both these factors within the framework of a self-consistent approach, undertaken by a number of authors,⁵ cannot be regarded as convincing (see the discussion given in Ref. 6). To elucidate the physics of the phenomenon and, in particular, of the possible conductivity mechanisms, it is therefore interesting to consider problems in which band formation

and scattering can be treated independently.

In this paper, we shall examine a $2D$ system whose Landau levels have broadened into bands as a result of magnetic breakdown. If the width of the magnetic band produced in this way is large in comparison with collisional level broadening Γ , the conductivity can be calculated from impurity scattering by perturbation theory.

We consider an inversion layer on the surface of a semiconductor with high Miller indices (Si—Ref. 12, InSb—Ref. 13). Since we have a long crystallographic period for translations along the surface, we can use the effective-mass approximation to introduce an additional weak one-dimensional periodic potential $V(x)$ with period A much greater than the lattice constant a . This superlattice gives rise to minigaps in the electron spectrum, and measurements of the size of these (1–20 meV) can be used to estimate the amplitude V_0 of the superlattice potential. As a rule, the bottom minigap $2V_0$ turns out to be small in comparison with the width $2\pi^2\hbar^2/mA^2$ of the ground allowed miniband, where m is the effective mass¹² (we confine our attention to minigaps that are unrelated to the intervalley interaction). The period A is determined by the crystallographic orientation of the surface and, as a rule, is equal to $a/2 \sin\theta$ for Si and $a/3^{1/2} \sin\theta$ for InSb, where $\theta \ll 1$ is the deviation of the surface under consideration from the basal plane [(100) for Si and (111) for InSb].

When a magnetic field \mathbf{B} perpendicular to the $2D$ layer is present, the superlattice potential lifts the degeneracy of the Landau level with respect to the center of the cyclotron orbit, and this may lead to the appearance of one-dimensional ($1D$) magnetic bands. The energy spectrum of such systems has been calculated in the three-dimensional ($3D$) case for various limiting situations.^{14–19} A symmetry classification of the states and an analysis of the spectrum for arbitrary B have also been reported.²⁰ Magnetic bands appear in studies

of magnetic breakdown in some metals and narrow band gaps on individual segments of the Fermi surface.²¹

The analysis given below is valid when the collisional broadening of Landau levels is small in comparison with the width of a magnetic band. The latter is very sensitive to the ratio of A to the magnetic length $\lambda = (\hbar c/eB)^{1/2}$. In weak fields, ($\lambda \gg A$), the bandwidth is exponentially small and the band itself is substantially "smeared out" by scattering (usually, $\Gamma \sim 1$ meV). The most interesting situation is that for which $\lambda \lesssim A$. When $\theta' 1^\circ - 3^\circ$ and $B = 0.5 \times 10^5 - 1.5 \times 10^5$ G, we have $A = 157 \text{ \AA} - 53 \text{ \AA}$ (Si), $A = 213 \text{ \AA} - 71 \text{ \AA}$ (InSb), and $\lambda = 115 \text{ \AA} - 66 \text{ \AA}$. It is clear that the condition

$$A/\lambda \sim 1, \quad (1)$$

can be realistically satisfied, and it may be expected that the magnetic band width will be small in comparison with Γ . It is important to remember that in such strong magnetic fields a real 2D system will be close to the magnetic quantum limit, and the quasiclassical analysis of magnetic breakdown^{21,22} will be invalid. It is thus clear that the determination of conductivity within the magnetic band is a topical quantum-mechanical problem.

A similar problem was solved in the 3D case. The situation typical of metals, in which the number of filled Landau levels is large, was analyzed in Ref. 23. The magnetoconductivity of 3D electrons in the presence of a superlattice was calculated numerically in Ref. 19. A decrease of the dimensionality of space alters radically the density of states (it has a 1D divergence at the band extrema), so that one can expect a considerable change in the behavior of the transport coefficients.

In this paper, we use the Kubo formula to calculate the diagonal components of the magnetoconductivity tensor of a 2D electron gas from the ground magnetic 1D band formed from the lowest Landau level. We shall concentrate our attention on case (1), which is not attained in 3D metals in realistic fields. The magnetic band is assumed to be narrow in comparison with the separation between the Landau levels, whose spin and valley degeneracy are neglected. Born scattering by short-range impurities of low-density n_i ($n_i \lambda^2 \ll 1$) is taken into account. The effective radius of these impurities is assumed to be small in comparison with all the characteristic lengths of the problem, so that we can use the δ -impurity approximation. The entanglement of Landau levels in the field of the impurity and superlattice potentials is neglected. The explicit form of $V(x)$ is not specified.

The spectrum and density of states are found in Sec. 2 and σ_{xx} and σ_{yy} are determined in Secs. 3 and 4. It is shown that there are two conductivity mechanisms, the classical due to band motion, and the quantum-mechanical due to migration of the center of the cyclotron orbit. The cumbersome calculations are relegated to Appendices 1-4. The main results and a discussion of the effects that may take us outside the framework of our approximations are presented in Sec. 5.

2. ENERGY SPECTRUM AND DENSITY OF STATES

Consider a 2D electron gas in the inversion layer on the $z = 0$ plane with high Miller indices. The effect of this sur-

face will be represented by the one-dimensional superlattice potential $V(x) = V(x + A)$. The electron Hamiltonian in the quantizing magnetic field $\mathbf{B} = (0, 0, B)$ in the presence of impurities producing short-range effects is

$$H = \frac{1}{2m} \left(\mathbf{p} + \frac{e}{c} \mathbf{A} \right)^2 + V(x) + U(\mathbf{r}), \quad U(\mathbf{r}) = u_0 \sum_i \delta(\mathbf{r} - \mathbf{r}_i),$$

where $\mathbf{p} = (p_x, p_y)$ is the momentum operator, $\mathbf{r}_i = (x_i, y_i)$ is the position vector of the i -th impurity, and $\mathbf{A} = (0, Bx, 0)$.

The potential $V(x)$ produces a partial removal of the degeneracy of the Landau levels with respect to the center of the orbit, and this results in the formation of 1D magnetic bands. We shall assume that the potential is weak. The wave functions of the Hamiltonian unperturbed by the impurities can be taken in the zero-order approximation in V :

$$\Psi_{Nk} = L^{-1/2} e^{iky} \Phi_N(x + \lambda^2 k), \quad (2)$$

whereas the spectrum can be taken in the first order in V :

$$\varepsilon_N(k) = (N + 1/2) \hbar \omega_c + \langle Nk | V | Nk \rangle, \quad (3)$$

where Φ_N is the Hermite function, N is the number of the Landau level, $\omega_c = eB/mc$ is the cyclotron frequency, $-\lambda^2 k$ is the x -coordinate of the center of the orbit, which is a good quantum number, and L is the normalizing length. The potential $V(x)$ is weak if the width of the magnetic band is small in comparison with $\hbar \omega_c$. The bandwidth depends on the rate at which $V(x)$ varies over lengths of the order of λ . Unfortunately, the explicit form of $V(x)$ is unknown, so that we shall consider two limiting cases for illustration. For a "smooth" superlattice²³

$$V(x) = V_0 \cos(2\pi x/A), \quad (4)$$

$$\varepsilon_N(k) = (N + 1/2) \hbar \omega_c + V_0 L_N(2\pi^2 \lambda^2/A^2) \exp(-\pi^2 \lambda^2/A^2) \cos(2\pi \lambda^2 k/A), \quad (5)$$

where L_N is a Laguerre polynomial with $L_0 = 1$. For an extremely "rough" superlattice, we use the Kronig-Penney potential:

$$V(x) = 1/2 V_0 A \sum_s \delta(x + sA),$$

$$\varepsilon_N(k) = (N + 1/2) \hbar \omega_c + 1/2 V_0 A \sum_s \Phi_N^2(sA + \lambda^2 k). \quad (6)$$

We shall confine our attention to the ground magnetic band with $N = 0$. Transforming the sum in (6) with the aid of the Poisson summation formula, we find that in a relatively weak magnetic field ($\pi^2 \lambda^2 \gg A^2$) the two expressions (6) and (5) differ only by a shift of the origin from which the energy is measured, and the half-width of the ground magnetic band

$$\Delta = V_0 \exp(-\pi^2 \lambda^2/A^2) \quad (7)$$

increases exponentially with increasing B . Further increase in B results in the saturation ($\Delta = V_0$) of the half-width of the ground band in model (5), whereas in model (6) in strong magnetic fields ($\lambda^2 \ll A^2$), the half-width continues to increase as $V_0 A [1 - 2 \exp(-A^2/4\lambda^2)]/4\pi^{1/2} \lambda$. In this limit, the spectrum (6) becomes asymmetric: the effective mass of electrons at the bottom of the ground band is

$$m_e^* = \frac{\pi^{1/2} \hbar^2 \lambda}{V_0 A^3} \exp\left(\frac{A^2}{4\lambda^2}\right)$$

and is much greater than the effective mass of "holes" near the top of this band

$$m_h^* = \pi^{1/2} \hbar^2 / V_0 A \lambda,$$

whereas in model (5) the spectrum is always symmetric.

The dispersion relation in the band, written in terms of the position of the center of the orbit $\lambda^2 k$, is periodic with A / λ^2 (Ref. 20), i.e.,

$$\varepsilon_N(k + A/\lambda^2) = \varepsilon_N(k).$$

Suppose that, within the interval $[-A/2\lambda^2, A/2\lambda^2]$, the equation $\varepsilon_N(k) = E$ has the roots $k^{(i)}$, $i = 1, 2, \dots$. The density of states in the N th magnetic band is then given by

$$\begin{aligned} N(E) &= \frac{1}{S} \sum_k \delta(E - \varepsilon_N(k)) \\ &= \frac{1}{2\pi \hbar A} \sum_i \frac{1}{|v^{(i)}|}, \end{aligned} \quad (8)$$

where $\hbar v^{(i)} = \partial \varepsilon_N / \partial k$ for $k = k^{(i)}$. The divergence of $N(E)$ at the band extrema (see Fig. 1a) is a consequence of the fact that $\varepsilon_N(k)$ is one-dimensional. In the model (5),

$$N(E) = 1/2\pi^2 \lambda^2 (\Delta^2 - E^2)^{1/2}, \quad (9)$$

and the electron density n_s in the ground magnetic band depends on the Fermi energy E_F as follows:

$$E_F = -\Delta \cos 2\pi^2 \lambda^2 n_s.$$

Here and below, whenever we use the model (5), the energy is

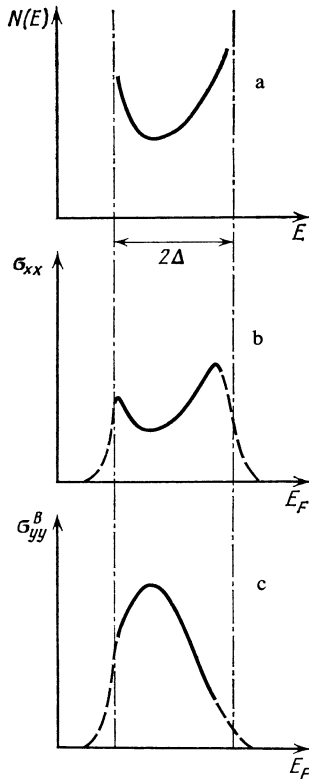


FIG. 1. a) Density of states in a magnetic band with two extrema; b) conductivity σ_{xx} in the direction of the superlattice axis; c) band contribution to the conductivity σ_{yy}^B across the superlattice axis. Dashed curves correspond to the inclusion of collisional broadening and the dot-dash curve shows the magnetic band edge.

measured from the ground Landau level.

We now give some numerical estimates for the inversion layer on the surface of Si. For $\theta = 1^\circ$, $V_0 = 10$ meV, and $B = 1.5 \times 10^5$ G, we have $A = 157 \text{ \AA}$, $\lambda = 66 \text{ \AA}$, $\hbar\omega_c \simeq 9.1$ meV and, in models (5) and (6), $2\Delta \simeq 3.5$ meV. The conditions for the appearance of the band spectrum (3) are then satisfied ($\hbar\omega_c \gg 2\Delta \gg \Gamma$) if $\Gamma \sim 1$ meV (Ref. 1), and at $n_s \lesssim 3.6 \times 10^{11} \text{ cm}^{-2}$ the system reaches the quantum limit. It is readily verified that $2\Delta / \hbar\omega_c \lesssim m V_0 A^2 / \pi^2 \hbar^2$ in the case of model (5), and the approximation defined by (2) and (3) is valid for all B provided the minigap width in the original (at $B = 0$) spectrum is small in comparison with the width of the allowed miniband. As noted in Sec. 1, it is precisely this case that is usually realized in experiments.

As N increases, the bandwidth decreases, and this complicates its experimental detection. Moreover, for $N > 0$, the variation of B may be accompanied by oscillations of the bandwidth, which are described by Laguerre polynomials in model (5). In other respects, however, the results obtained below in the quantum limit do not change qualitatively as the higher-lying magnetic bands become filled.

3. CONDUCTIVITY IN THE DIRECTION OF THE SUPERLATTICE AXIS

Let us now calculate the diagonal components of the conductivity tensor σ_{xx} corresponding to a current along the superlattice axis. An electron moving along the y axis with velocity $\sim \partial \varepsilon / \partial k$ is scattered by an impurity and is displaced in the direction of the x axis along the electric field. The conductivity σ_{xx} is determined by migration, due to scattering by impurities, of the center of the cyclotron orbit of the electron. This is typical of transverse conductivity in a magnetic field in the 3D case.²⁴

The calculation was based on the Kubo formula in the representation of the orbit center²⁴:

$$\sigma_{xx} = \frac{e^2 \hbar}{\pi S} \int dE \left(-\frac{\partial f}{\partial E} \right) \langle \text{Sp } X \text{ Im } G(E) X \text{ Im } G(E) \rangle, \quad (10)$$

where $X = i\lambda^2 \partial / \partial y$ is the operator for the x coordinate of the center of the orbit, $G(E) = (E - H + i0)^{-1}$ is a single-particle Green function, $f(E)$ is the Fermi-Dirac function, S is the area of the system, and the angle brackets denote standard averaging over impurity configurations.²⁵

The use of (10) is justified because the relative coordinate of the electron on the cyclotron orbit is bounded. The much more complicated calculation based on the complete Kubo formula²⁶ leads to the same result.

The operator representing the velocity of the center of the orbit, $X_{\alpha\alpha'} = i\hbar^{-1}(X_\alpha - X_{\alpha'})U_{\alpha\alpha'}$, is linear in U , so that we confine our attention in (10) to the lowest order in scattering, which entitles us to replace $G(E)$ with the unperturbed Green function $G^0_{\alpha\alpha'} = \delta_{\alpha\alpha'}(E - \varepsilon_\alpha + i0)^{-1}$, where $\alpha = \{Nk\}$ is the set of quantum numbers and $X_\alpha = -\lambda^2 k$. In basis (2) we have at $T = 0$

$$\sigma_{xx} = \frac{\pi \hbar e^2}{S} \sum_{\alpha\alpha'} \langle |X_{\alpha\alpha'}|^2 \rangle \delta(E_F - \varepsilon_\alpha) \delta(E_F - \varepsilon_{\alpha'}), \quad (11)$$

$$\langle |\dot{X}_{\alpha\alpha'}|^2 \rangle = \frac{n_i u_0^2 \lambda^2 (k - k')^2}{(2\pi)^{1/2} \hbar^2 L} \times \left[(2\pi)^{1/2} \lambda \int \Phi_{N'}^2(x + \lambda^2 k) \Phi_{N'}^2(x + \lambda^2 k') dx \right]. \quad (12)$$

In the quantum limit ($N = N' = 0$), the expression in the square brackets in (12) is equal to $\exp[\lambda^2(k - k')^2/2]$ and (11) becomes simpler. Leaving out the laborious though straightforward intermediate steps, and merely quote the final result:

$$\sigma_{xx}(E_F) = \frac{e^2}{2\pi \hbar A} \sum_j \frac{1}{|v_F^{(j)}|} \times \left[\frac{n_i u_0^2 A^2}{2^{1/2} \pi^{3/2} \hbar^2 \lambda} \sum_i \frac{1}{|v_F^{(i)}|} F_1 \left(\frac{2\pi \lambda^2 (k_F^{(j)} - k_F^{(i)})}{A} \right) \right], \quad (13)$$

where the function $F_1(b)$ is determined in Appendix 1, i and j label the roots of the equation $\varepsilon(k) = E_F$ on the period of $\varepsilon(k)$, and $v_F^{(j)} = v^{(j)}$ for $E = E_F$. In the region of magnetic fields defined by (1), in which we are interested, we find that condition (A.3) is satisfied for $F_1(b)$, the asymptotic behavior described by (A.4) is valid, and σ_{xx} satisfies the Einstein relation

$$\sigma_{xx}(E_F) = e^2 N(E_F) [(\pi n_i u_0^2 \lambda^2 / \hbar) N(E_F)]. \quad (14)$$

The density of states at the Fermi level in this expression is given by (8), and the expression in the square brackets can be interpreted as the coefficient of diffusion $D_{xx}(E_F)$ for the center of the orbit along the x axis.

The function $\sigma_{xx}(E_F)$ follows the variation of $N^2(E_F)$. The divergence of σ_{xx} at the band extrema ($v_F^{(j)} \rightarrow 0$) is determined by two factors, namely, the divergence of $N(E_F)$ and the divergence of the diffusion coefficient $D_{xx}(E_F)$. It is well known that the latter is due^{24,27} to the use of the Born approximation to calculate the probability $W_{\alpha\alpha'}$ of the elastic scattering:

$$W_{\alpha\alpha'} = \frac{2\pi}{\hbar} \langle |U_{\alpha\alpha'}|^2 \rangle \delta(\varepsilon_{\alpha} - \varepsilon_{\alpha'}). \quad (15)$$

To cut off the divergence of σ_{xx} , we must, as in the 3D case, take into account the smearing of $N(E_F)$ by collisions,²⁸ or abandon the Born approximation.^{29,30} Other possible cut-off mechanisms (inelasticity of the scattering,³¹ allowance for the finite electric field³²) will not be considered here.

Let us now consider the collisional cutoff mechanism and confine our attention to model (5) for the sake of simplicity. We then find that (9) and, consequently, (14) diverge at the band edges (see Figs. 1a and 1b). As E_F approaches the band edges, expression (14) becomes meaningless at $|E_F| \gtrsim |E_{F1}|$, where $|E_{F1}|$ is given by

$$\Delta - |E_{F1}| = \hbar / \tau(E_{F1}). \quad (16)$$

When $|E_F| \gtrsim |E_{F1}|$, the interaction between the electrons and the scattering impurities cannot be resolved into individual collisions.²⁸ The time τ between collisions is determined with the aid of (15) and, in the quantum limit, is given by

$$\frac{1}{\tau(E_F)} = \sum_{\mathbf{k}} W_{0\mathbf{k},0\mathbf{k}} = \frac{n_i u_0^2}{(2\pi)^{1/2} \hbar^2 \lambda |v_F|} \left[F_2 \left(\frac{4\pi \lambda^2 k_F}{A} \right) + F_2(0) \right]. \quad (17)$$

When the function $F_2(b)$ is given by the limiting formula (A.3) in Appendix 1, we have the asymptotic expression (A.5) and instead of (17) we obtain

$$1/\tau(E_F) \approx n_i u_0^2 / \pi \hbar \lambda^2 (\Delta^2 - E_F^2)^{1/2}. \quad (18)$$

Simultaneous solution of (16) and (18) subject to the condition $\hbar/\tau \ll \Delta$ yields

$$(\Delta - |E_{F1}|) / \Delta \approx (n_i u_0^2 / 2^{1/2} \pi \lambda^2 \Delta^2)^{2/3} \ll 1. \quad (19)$$

Apart from numerical coefficients, the last inequality can be written in the form $(\Gamma/\Delta)^{4/3} \ll 1$ where $\Gamma = (2n_i u_0^2 / \pi \lambda^2)^{1/2}$ is the broadening of the Landau level in the self-consistent Born approximation.⁵ As scattering increases, $|E_{F1}|$ shifts toward the center of the band and the range of validity of (14) becomes smaller and shrinks to zero when (19) is not satisfied.

On the other hand, as E_F approaches the band edges, $|v_F|$ falls, and there is more intensive scattering of electrons by impurities. At $|E_F| \gtrsim |E_{F2}|$, the Born approximation becomes unsuitable and scattering by each impurity must be taken into account in all perturbation theory orders^{29,30} (see Appendix 2). The quantity $|E_{F2}|$ in (A.8) is close to the band edge if $(u_0 |2\pi \lambda^2 \Delta|)^2 \ll 1$.

It is thus clear that (14) is valid for

$$|E_F| < E_F^m = \min \{|E_{F1}|, |E_{F2}|\}.$$

The function $\sigma_{xx}(E_F)$ in model (5) has two peaks at the band edges (Fig. 1b). As B is reduced, the width Δ decreases exponentially, the peaks $\sigma_{xx}(\pm E_F^m)$ come closer together, the σ_{xx} valley at the band center is reduced, and, finally, the valley disappears altogether for $E_F^m \ll \Delta$. The above results are then no longer valid, and the problem reduces to the evaluation of the 2D magnetoconductivity without the sublattice. The intensification of scattering is qualitatively equivalent to a reduction in B .

The above results are readily extended to the case $T \neq 0$. In the quantum limit, and not too high a temperature ($T \ll \hbar \omega_c$) we have

$$\sigma_{xx}(T) = \int dE (-\partial f / \partial E) \sigma_{xx}(E), \quad (20)$$

where $\sigma_{xx}(E)$ is given by (14) and the integral is evaluated over the entire band, taking into account the cutoff at the band extrema. For example, in model (5), the finite value of T for $T \ll \Delta$ gives a small ($\sim T^2/\Delta^2$) positive correction to (14). For $T \gg \Delta$, the chemical potential μ depends on the degree of filling of the band $\nu = 2\pi \lambda^2 n_s$ as follows:

$$1 + \exp(-\mu/T) = 1/\nu$$

which is valid to within terms of the order of Δ/T . With the same precision, we find from (20) that

$$\sigma_{xx}(T) = \nu(1-\nu) \frac{e^2}{2\pi^2 \hbar} \frac{n_i u_0^2}{2\pi \lambda^2 \Delta^2} \frac{\Delta}{T} \ln \left| \frac{\Delta + E_F^m}{\Delta - E_F^m} \right|. \quad (21)$$

When $T \gg \Delta$, the conductivity falls, since the band is, on an aver-

age, uniformly filled with electrons because of the temperature smearing.

4. CONDUCTIVITY IN THE DIRECTION PERPENDICULAR TO THE SUPERLATTICE AXIS

The conductivity component σ_{yy} will now be calculated from the Kubo formula (10) with the replacement $\dot{X} \rightarrow \dot{Y}$. The operator of the orbit-center velocity along the y axis is

$$\dot{Y} = \frac{i}{\hbar} [H, Y] = -\frac{\lambda^2}{\hbar} \frac{\partial U}{\partial x} - \frac{\lambda^2}{\hbar} \frac{\partial V}{\partial x}, \quad (22)$$

where $Y = -i\lambda^2 \partial / \partial x + y$ contains two contributions. The first ($\sim \partial U / \partial x$) is proportional to the force acting on the electron due to the impurities, and the second ($\sim \partial V / \partial x$) is due to the superlattice. Hence, σ_{yy} is determined both by migration of the center of the orbit during scattering by impurities and by classical motion of the electron within the magnetic band. Since σ_{yy} is bilinear in \dot{Y} , cross terms containing $(\partial V / \partial x)(\partial U / \partial x)$ may, in principle, appear. However, it is shown in Appendix 3 that these terms vanish when on averaging over the impurities.

Thus, $\sigma_{yy} = \sigma_{yy}^M + \sigma_{yy}^B$ where the migration σ_{yy}^M and band σ_{yy}^B contributions are given by the following expressions for $T = 0$:

$$\sigma_{yy}^M = \frac{e^2 \lambda^4}{\pi \hbar S} \left\langle \text{Sp} \frac{\partial U}{\partial x} \text{Im} G(E_F) \frac{\partial U}{\partial x} \text{Im} G(E_F) \right\rangle, \quad (23)$$

$$\sigma_{yy}^B = \frac{e^2 \lambda^4}{\pi \hbar S} \left\langle \text{Sp} \frac{\partial V}{\partial x} \text{Im} G(E_F) \frac{\partial V}{\partial x} \text{Im} G(E_F) \right\rangle. \quad (24)$$

Let us now consider the migration contribution to σ_{yy} . Evaluation of σ_{yy}^M is analogous to the evaluation of σ_{xx} . Since

$$\left\langle \left| \left(\frac{\partial U}{\partial x} \right)_{\alpha\alpha'} \right|^2 \right\rangle = \frac{n_i u_0^2}{L} \int \left\{ \frac{d}{dx} [\Phi_N(x + \lambda^2 k) \Phi_{N'}(x + \lambda^2 k')] \right\}^2 dx,$$

we find from (23) that, in the lowest order in scattering and in the quantum limit,

$$\sigma_{yy}^M(E_F) = \frac{e^2}{2\pi \hbar A} \sum_j \frac{1}{|v_F^{(j)}|} \times \left[\frac{n_i u_0^2 \lambda}{2^{1/2} \pi^{1/2} \hbar^2} \sum_i \frac{1}{|v_F^{(i)}|} F_2 \left(\frac{2\pi \lambda^2 (k_F^{(i)} - k_F^{(j)})}{A} \right) \right]. \quad (25)$$

In the limit defined by (A.3), this formula is identical with (14), with the expression in the square brackets in (25) becoming the diffusion coefficient $D_{yy}(E_F)$ of the center of the electron orbit in the direction of the y axis. We then have $D_{yy}(E_F) \approx D_{xx}(E)$, and all the conclusions of Sect. 3 apply also to σ_{yy}^M . The diffusion becomes anisotropic in very strong magnetic fields and $\sigma_{yy}^M(E_F) \neq \sigma_{xx}(E_F)$.

Let us now calculate the band contribution to σ_{yy} . We shall confine our attention to the ground band and will omit the index $N = 0$. Since

$$\left(\frac{\partial V}{\partial x} \right)_{k,k'} = \frac{1}{\lambda^2} \frac{\partial \varepsilon(k)}{\partial k} \delta_{k,k'},$$

we can rewrite (24) in the form

$$\sigma_{yy}^B = \frac{e^2}{\pi \hbar S} \sum_{k,k'} \left\langle \frac{\partial \varepsilon(k)}{\partial k} \text{Im} G_{k,k'}(E_F) \times \frac{\partial \varepsilon(k')}{\partial k'} \text{Im} G_{k',k}(E_F) \right\rangle. \quad (26)$$

Computational difficulties that arise when we try to "unravel" (26) in the general case have the same origin as the difficulties encountered in the solution of the Boltzmann equation for arbitrary $\varepsilon(k)$. Let us therefore consider a very simple "Fermi surface" $\varepsilon(k) = E_F$ consisting of the two points k_F and $-k_F$ within the period of the function $\varepsilon(k)$. The next steps are analogous to the determination of the conductivity of a free electron gas under elastic scattering by impurities.³³ The calculation is carried out in Appendix 4 with allowance for the specific features of the spectrum $\varepsilon(k)$ (umklapp processes must be taken into account).

The result

$$\sigma_{yy}^B(E_F) = e^2 N(E_F) v_F^2 \left[\frac{(2\pi)^{1/2} \hbar^2 \lambda |v_F|}{2n_i u_0^2} F_2^{-1} \left(\frac{4\pi \lambda^2 k_F}{A} \right) \right] \quad (27)$$

describes the classical conductivity of a degenerate electron gas in a one-dimensional band $\varepsilon(k)$. The expression in the square brackets in (27) can readily be shown to be the transport relaxation time. In the limit defined by (A.3), it follows from (8), (27), and (A.5) that

$$\sigma_{yy}^B(E_F) = \frac{e^2 \hbar}{2\pi n_i u_0^2} v_F^2. \quad (28)$$

The band conductivity σ_{yy}^B , in contrast to migration conductivity σ_{yy}^M , increases as scattering is reduced. The behavior of $\sigma_{yy}^B(E_F)$ is determined by the function $v_F^2(E_F)$ (see Fig. 1c). Scattering increases at the band extrema and (28) becomes invalid. The range of validity of (28) is reduced with increasing scattering, and eventually vanishes altogether. In model (5) this occurs for $E_F^m \ll \Delta$, (see Sect. 3).

When $T \neq 0$, the conductivity $\sigma_{yy}(T)$ is given by (20) with the replacement $x \rightarrow y$. Thus, as the temperature increases in model (5), the conductivity σ_{yy}^B first decreases like $-T^2/\Delta^2$ but for large T ($\Delta \ll T \ll \hbar\omega_c$) it assumes the form

$$\sigma_{yy}^B(T) = \nu(1-\nu) \frac{e^2}{\hbar} \frac{2\pi \lambda^2 \Delta^2}{n_i u_0^2} \frac{4\lambda^2}{3A^2} \frac{\Delta}{T}. \quad (29)$$

Comparison of σ_{yy}^M and σ_{yy}^B shows that the main contribution to σ_{yy} (at any rate, well away from the band extrema) is due to σ_{yy}^B . It follows that the conductivity is highly anisotropic in this system and $\sigma_{xx} \ll \sigma_{yy}$.

5. DISCUSSION OF RESULTS

Conduction in the inversion layer on a semiconductor surface with high Miller indices is produced by two mechanisms. One of them is due to the migration of the center of the cyclotron orbit as a result of scattering by impurities, and contributes to both σ_{xx} and σ_{yy} . The other is due to classical scattering during the motion of an electron within a magnetic band, and contributes only to the conductivity σ_{yy} in the direction perpendicular to the superlattice axis. As scattering is reduced, the conductivity due to the first mechanism is reduced, and that due to the second increased. The presence of two conduction mechanisms does not appear to be confined to this particular system. For example, similar contri-

butions are found in the 3D case. This was noted in Refs. 21 and 23 where a study was reported of coherent magnetic breakdown. It is likely that they will also be found in inversion layers on ordinary (low Miller index) semiconductor surfaces.

The width of the magnetic band increases exponentially with increasing B , so that strong magnetic fields are necessary for the experimental detection of the above effects. For an inversion layer on a surface at the angle $\theta \sim 1^\circ$ to the (100) plane of Si or the (111) plane of InSb in a field of $B \sim 1.5 \times 10^5$ G, the width of the ground magnetic band exceeds 1 meV, and the conditions for the formation of the band may be satisfied in sufficiently pure specimens ($\Gamma < 1$ meV).

There has been a report^{1,12} of measurements of intervalley magnetic breakdown in inversion layers, but they were performed in relatively weak magnetic fields ($\lambda \gg A$) for which the conditions for the formation of the magnetic band were not satisfied.

In magnetic fields that are strong enough for inequality (A.3) to be reversed, the overlap of wave functions is sharply reduced, and the degree of anisotropy in conductivity is increased still further. However, the conditions for the validity of our results [see, for example, (19)] may then no longer be satisfied. The necessity for including multicenter scattering is an indirect indication of the tendency of electronic states to localize. In actual fact, a system placed in sufficiently strong B constitutes a set of weakly coupled "filaments" running along the y axis. The possibility of localization in this quasi-one-dimensional case is well known.³⁴

In very pure specimens, the homogeneity of the spectrum (3) and the associated "pointlike" Fermi surface may lead to an instability of the system to formation of a charge-density wave whose wave vector q_y is commensurate with the separation between the "Fermi points" and, in particular, with the period of the function $\varepsilon(k)$. The nature of the ground state under these conditions requires separate analysis. Here we merely note that if the charge-density wave is in fact produced the spectrum becomes two-dimensional, and the conditions for the observation of the unusual quantization of σ_{xy} predicted in Ref. 35 may be satisfied.

Effects typical of narrow allowed-band crystals may appear in a strong electric field F (Ref. 36). For example, at $F = (0, F)$ the electron will oscillate in the band with frequency $\omega = 2\pi cF/AB$ (the analog of the Wannier-Stark frequency). This should be reflected in the properties of the transport coefficients (cf. Ref. 21).

The above discussion indicates the potential productivity of galvanomagnetic phenomena in the system that we have considered, and we hope will act as stimulus to experimental studies.

The authors are grateful to V. B. Sandomirskiĭ for his interest in this research and for valuable suggestions, and to M. I. Kaganov and R. A. Suris for fruitful discussions.

APPENDIX 1

The following two series are frequently encountered in calculations:

$$F_1(b) = \sum_{n=-\infty}^{\infty} (b+2\pi n)^2 \exp\left\{-\frac{A^2(b+2\pi n)^2}{8\pi^2\lambda^2}\right\}, \quad (\text{A.1})$$

$$F_2(b) = \sum_{n=-\infty}^{\infty} \exp\left\{-\frac{A^2(b+2\pi n)^2}{8\pi^2\lambda^2}\right\}, \quad (\text{A.2})$$

where $0 \leq b < 2\pi$. They can be transformed with the aid of the Poisson formula:

$$F_1(b) = \frac{4(2\pi)^{1/2}\pi^2\lambda^3}{A^3} \sum_{p=-\infty}^{\infty} e^{ipb} \left(1 - \frac{4\pi^2\lambda^2 p^2}{A^2}\right) \exp\left(-\frac{2\pi^2\lambda^2 p^2}{A^2}\right)$$

$$F_2(b) = \frac{(2\pi)^{1/2}\lambda}{A} \sum_{p=-\infty}^{\infty} e^{ipb} \exp\left\{-\frac{2\pi^2\lambda^2 p^2}{A^2}\right\}. \quad (\text{A.3})$$

When

$$A^2/2\pi^2\lambda^2 \ll 1$$

we retain only terms with $p = 0$ in the above sums:

$$F_1(b) \approx 4(2\pi)^{1/2}\pi^2\lambda^3/A^3, \quad (\text{A.4})$$

$$F_2(b) \approx (2\pi)^{1/2}\lambda/A. \quad (\text{A.5})$$

It is clear that (A.3) and (A.4) are valid for (1). In the limit of very strong fields ($2\lambda^2/A^2 \ll 1$), only the first few terms need be retained in (A.1) and (A.2). In the intermediate region ($1/2\pi^2 < \lambda^2/A^2 < 1/2$), the two asymptotic forms give very similar results.

APPENDIX 2

The precise scattering amplitude $t_{\alpha\alpha'}(E)$ for an isolated impurity $u = u_0\delta(\mathbf{r} - \mathbf{r}_i)$ has the form of the series^{29,30}

$$t_{\alpha\alpha'}(E) = u_{\alpha\alpha'} + \sum_{\beta} \frac{u_{\alpha\beta}u_{\beta\alpha'}}{E - \varepsilon_{\beta} + i0}$$

$$+ \sum_{\beta\gamma} \frac{u_{\alpha\beta}u_{\beta\gamma}u_{\gamma\alpha'}}{(E - \varepsilon_{\beta} + i0)(E - \varepsilon_{\gamma} + i0)} + \dots,$$

which is readily summed:

$$t_{\alpha\alpha'}(E) = u_0 \Psi_{Nk}^*(\mathbf{r}_i) \Psi_{N'k'}(\mathbf{r}_i) \frac{1}{1 - K(E)}, \quad (\text{A.6})$$

where

$$K(E) = u_0 \sum_{Nk} |\Psi_{Nk}(\mathbf{r}_i)|^2 \frac{1}{E - \varepsilon_N(k) + i0}.$$

In the quantum-mechanical limit, neglecting the entanglement of the Landau levels for model (5),

$$K(E) = \frac{u_0}{2\pi^{1/2}\lambda} \int_{-\infty}^{\infty} e^{-\lambda^2 k^2} \frac{dk}{E - \varepsilon(k) + i0} = \frac{u_0 A}{4\pi^{5/2}\lambda^3}$$

$$\times \sum_{p=-\infty}^{\infty} \int_{-\pi}^{\pi} \exp\left[-\frac{A^2(t+2\pi p)^2}{4\pi^2\lambda^2}\right] \frac{dt}{E - \Delta \cos t + i0} \quad (\text{A.7})$$

$$\approx -\frac{i u_0}{2\pi\lambda^2 (\Delta^2 - E^2)^{1/2}}.$$

The sum in (A.7) was evaluated with the aid of (A.3).

Substituting (A.7) in (A.6), we find that the Born approximation is inadequate at $|E| \gtrsim |E_{F2}|$, where E_{F2} is given by the condition $|K(E_{F2})| = 1$. Hence,

$$|E_{F2}| = \left[\Delta^2 - \left(\frac{u_0}{2\pi\lambda^2}\right)^2\right]^{1/2}. \quad (\text{A.8})$$

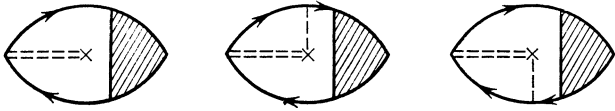


FIG. 2. Diagrams for the cross term in (A.9). Dashed single lines and double lines correspond to respective interaction of $u_{\alpha\alpha'}$ and $(\partial u/\partial x)\delta_{\alpha\alpha'}$ with the impurity.

APPENDIX 3

When (22) is substituted in the Kubo formula, the cross terms are proportional to

$$\left\langle \text{Sp} \frac{\partial U}{\partial x} \text{Im} G(E_F) \frac{\partial V}{\partial x} \text{Im} G(E_F) \right\rangle. \quad (\text{A.9})$$

In our scattering approximations, averaging over the impurity configurations in (A.9) leads to the diagrams shown in Fig. 2 (Refs. 33 and 37), where the solid lines correspond to single-particle Green functions $\bar{G}_{\alpha\alpha'} = \bar{G}_{\alpha\alpha'} \delta_{\alpha\alpha'}$ in the Born approximation averaged over the impurities, and the vertex part $\Gamma_{\alpha\alpha'} = \Gamma_{\alpha} \delta_{\alpha\alpha'}$ satisfies the Dyson equation in Fig. 3a. The contribution of these diagrams is equal to zero because the following expressions appear in the course of their evaluation:

$$\int \left(\frac{\partial u}{\partial x} \right)_{\alpha\alpha'} d\mathbf{r}_i \infty \int dx \frac{d}{dx} [\Phi_N(x+\lambda^2 k) \Phi_{N'}(x+\lambda^2 k')] = 0,$$

$$\int \left(\frac{\partial u}{\partial x} \right)_{\alpha\alpha'} u_{\alpha'\alpha} d\mathbf{r}_i$$

$$\infty \int dx \frac{d}{dx} [\Phi_{N^2}(x+\lambda^2 k) \Phi_{N^2}(x+\lambda^2 k')] = 0.$$

APPENDIX 4

Averaging over impurities in (26) within the framework of standard approximations³³ leads to the following expression which corresponds to the diagram of Fig. 3b:

$$\sigma_{\nu\nu'}^B(E_F) = \frac{e^2}{4\pi\hbar S} \sum_k \frac{\partial \varepsilon(k)}{\partial k} \bar{G}_k(E_F+) \bar{G}_k(E_F-) \Gamma_k(E_F+, E_F-),$$

$$\bar{G}_k(E_F\pm) = (E_F - \varepsilon(k) \pm i\hbar/2\tau)^{-1}, \quad (\text{A.10})$$

where τ is given by (17) and Γ_k is the vertex part satisfying the Dyson equation of Fig. 3a:

$$\Gamma_k(E, E') = \frac{\partial \varepsilon(k)}{\partial k} + \sum_{k'} \langle |U_{k,k'}|^2 \rangle \bar{G}_{k'}(E) \bar{G}_{k'}(E') \Gamma_{k'}(E, E'). \quad (\text{A.11})$$

We now recognize that \bar{G}_k in (A.10) and (A.11), to within $i\hbar/2\tau$, has poles at $k = \pm k_F + (A/\lambda^2)p$, $p = 0, \pm 1, \dots$. It follows from (A.11) that $\Gamma_{k+A/\lambda^2} = \Gamma_k$, $\Gamma_{-k} = -\Gamma_k$ and

$$\Gamma_{k_F}(E_F+, E_F-) = \frac{1}{2} \hbar |v_F| \left[1 + F_2(0)/F_2 \left(\frac{4\pi\lambda^2 k_F}{A} \right) \right]. \quad (\text{A.12})$$

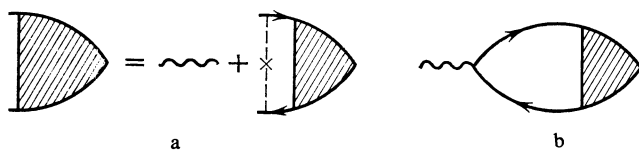


FIG. 3. Dyson equation for the vertex part (a) and the band contribution $\sigma_{\nu\nu'}^B$ (b). The wavy line represents the factor $(\partial \varepsilon_{\alpha}/\partial k)\delta_{\alpha\alpha'}$.

Here, we have taken into account the fact that

$$\int_0^{A/2\lambda^2} \bar{G}_k(E_F+) \bar{G}_k(E_F-) dk$$

$$= \frac{(2\pi)^{3/2} \lambda}{n_i u_0^2} \left[F_2(0) + F_2 \left(\frac{4\pi\lambda^2 k_F}{A} \right) \right]^{-1}. \quad (\text{A.13})$$

By substituting (A.12) in (A.10), and using (A.13), we obtain (27).

- ¹T. Ando, A. B. Fowler, and F. Stern, *Rev. Mod. Phys.* **54**, 437 (1982).
- ²K. Von Klitzing, G. Dorda, and M. Pepper, *Phys. Rev. Lett.* **45**, 494 (1980).
- ³B. A. Tavger and M. Sh. Erukhimov, *Zh. Eksp. Teor. Fiz.* **51**, 528 (1966) [*Sov. Phys. JETP* **24**, 354 (1967)].
- ⁴V. I. Ryzhii, *Fiz. Tekh. Poluprovodn.* **3**, 1704 (1969) [*Sov. Phys. Semicond.* **3**, 1432 (1969)].
- ⁵T. Ando and Y. Uemura, *J. Phys. Soc. Jpn.* **36**, 959 (1974); T. Ando, *J. Phys. Soc. Jpn.* **36**, 1521 (1974); **37**, 622, 1233 (1974).
- ⁶E. M. Baskin, L. I. Magarill, and M. V. Entin, *Zh. Eksp. Teor. Fiz.* **75**, 723 (1978) [*Sov. Phys. JETP* **48**, 365 (1978)].
- ⁷R. E. Prange, *Phys. Rev. B* **23**, 4802 (1981).
- ⁸H. Aoki and T. Ando, *Solid State Commun.* **38**, 1079 (1981).
- ⁹S. V. Iordansky, *Solid State Commun.* **43**, 1 (1982).
- ¹⁰N. A. Usov and F. R. Ulinich, *Zh. Eksp. Teor. Fiz.* **86**, 644 (1984) [*Sov. Phys. JETP* **59**, 376 (1984)].
- ¹¹D. E. Khmel'nitskiĭ, *Pis'ma Zh. Eksp. Teor. Fiz.* **38**, 454 (1983) [*JETP Lett.* **38**, 552 (1983)].
- ¹²V. A. Volkov, V. A. Petrov, and V. B. Sandomirskiĭ, *Usp. Fiz. Nauk* **131**, 423 (1980) [*Sov. Phys. Usp.* **23**, 375 (1980)].
- ¹³T. Eveltbaumer, U. Merkt, and J. P. Kotthaus, *Physica (Utrecht)* **BC1171-118**, 670 (1983).
- ¹⁴P. G. Harper, *Proc. Phys. Soc. London Sect. A* **68**, 874, 879 (1955).
- ¹⁵G. E. Zil'berman, *Zh. Eksp. Teor. Fiz.* **32**, 296 (1957) [*Sov. Phys. JETP* **5**, 208 (1957)]. **33**, 387 (1957) [*Sov. Phys. JETP* **6**, 299 (1958)].
- ¹⁶R. Tsu and J. Janak, *Phys. Rev. B* **9**, 404 (1974).
- ¹⁷K. Nakao, *J. Phys. Soc. Jpn.* **46**, 1669 (1979).
- ¹⁸I. A. Chaikovskii, G. M. Shmelev, and N. A. Enaki, *Phys. Status Solidi B* **108**, 559 (1981).
- ¹⁹T. Ando, *J. Phys. Soc. Jpn.* **47**, 1595 (1979).
- ²⁰A. M. Berezhevskii and R. A. Suris, *Zh. Eksp. Teor. Fiz.* **86**, 193 (1984) [*Sov. Phys. JETP* **59**, 109 (1984)].
- ²¹M. I. Kaganov and A. A. Slutskin, *Phys. Rep.* **98**, 189 (1983).
- ²²R. W. Stark and L. M. Falicov, *Prog. Low Temp. Phys.* **5**, 235 (1967).
- ²³H. Shiba and H. Fukuyama, *J. Phys. Soc. Jpn.* **26**, 910 (1969).
- ²⁴R. Kubo, S. Miyake, and N. Hashitsume, *Solid State Phys.* **17**, 269 (1965).
- ²⁵W. Kohn and J. Luttinger, *Phys. Rev.* **108**, 590 (1957).
- ²⁶R. Kubo, *J. Phys. Soc. Jpn.* **12**, 570 (1957).
- ²⁷E. Adams and T. Holstein, *J. Phys. Chem. Solids* **10**, 254 (1959).
- ²⁸B. I. Davydov and I. I. Pomeranchuk, *Zh. Eksp. Teor. Fiz.* **9**, 1294 (1939).
- ²⁹V. G. Skobov, *Zh. Eksp. Teor. Fiz.* **37**, 1467 (1959) [*Sov. Phys. JETP* **10**, 1039 (1960)]; **38**, 1304 (1960) [**11**, 941 (1960)].
- ³⁰Yu. A. Bychkov, *Zh. Eksp. Teor. Fiz.* **39**, 689 (1960) [*Sov. Phys. JETP* **12**, 483 (1961)].
- ³¹V. L. Gurevich and Yu. A. Firsov, *Zh. Eksp. Teor. Fiz.* **40**, 198 (1961) [*Sov. Phys. JETP* **13**, 137 (1961)].
- ³²L. I. Magarill and S. K. Savvinykh, *Zh. Eksp. Teor. Fiz.* **57**, 2079 (1969) [*Sov. Phys. JETP* **30**, 1128 (1970)]; **60**, 175 (1971) [**33**, 97 (1971)].
- ³³A. A. Abrikosov, L. P. Gor'kov, and I. E. Dzyaloshinskiĭ, *Metody kvantovoi teorii polya v statisticheskoi fizike (Methods of Quantum Field Theory in Statistical Physics)* GIFML, Moscow, 1962, p. 423 [English transl. Prentice Hall, 1963].
- ³⁴I. M. Lifshitz, S. A. Gredeskul, and L. A. Pastur, *Vvedenie v teoriyu neuporyadochennykh sistem (Introduction to the Theory of Disordered Systems)*, Nauka, Moscow, 1982, Chap. 3.
- ³⁵D. J. Thouless, M. Kohmoto, M. P. Nightingale, and M. den Nijs, *Phys. Rev. Lett.* **49**, 405 (1982).
- ³⁶A. Ya. Shik, *Fiz. Tekh. Poluprovodn.* **8**, 1841 (1974) [*Sov. Phys. Semicond.* **8**, 1195 (1974)].
- ³⁷H. Shiba, K. Kanda, H. Hasegawa, and H. Fukuyama, *J. Phys. Soc. Jpn.* **30**, 972 (1971).

Translated by S. Chomet